ACS APPLIED MATERIALS & INTERFACES

Research Article

www.acsami.org

Improved Dielectric Properties of Nanocomposites Based on Poly(vinylidene fluoride) and Poly(vinyl alcohol)-Functionalized Graphene

Dongrui Wang,[†] Yaru Bao,[†] Jun-Wei Zha,[†] Jun Zhao,[†] Zhi-Min Dang,[†,*] and Guo-Hua Hu[‡,*]

[†]Department of Polymer Science and Engineering, School of Chemistry and Biological Engineering, University of Science and Technology Beijing, Beijing, 100083, P. R. China

[‡]CNRS-Université de Lorraine, Laboratoire Réactions et Génie des Procédés, UPR3349, ENSIC, 1 rue Grandville, BP 20451, Nancy, F-54000, France

Supporting Information

ABSTRACT: In this work, two series of nanocomposites of poly(vinylidene fluoride) (PVDF) incorporated with reduced graphene oxide (rGO) and poly(vinyl alcohol)-modified rGO (rGO-PVA) were fabricated using solution-cast method and their dielectric properties were carefully characterized. Infrared spectroscopy and atom force microscope analysis indicated that PVA chains were successfully grafted onto graphene through ester linkage. The PVA functionalization of graphene surface can not only prevent the agglomeration of original rGO but also enhance the interaction between PVDF and rGO-PVA. Strong hydrogen bonds and charge transfer effect between rGO-PVA and PVDF were determined by infrared and Raman spectroscopies. The dielectric properties of rGO-PVA/PVDF and rGO/PVDF nanocomposites were investigated in a frequency range from 10^2 Hz to 10^7 Hz. Both composite systems exhibited an insulator-to-conductor percolating transition as the increase of the filler content. The percolation thresholds were estimated to be 2.24 vol % for rGO-PVA/PVDF composites and 0.61 vol % for rGO/PVDF composites, respectively. Near the percolation threshold, the dielectric permittivity of the nanocomposites was significantly promoted, which can be well explained by interfacial polarization effect and microcapacitor model. Compared to rGO/PVDF composites, higher dielectric constant and lower loss factor were simultaneously achieved in rGO-PVA/PVDF nanocomposites at a frequency range lower than 1×10^3 Hz. This work provides a potential design strategy based on graphene interface engineering, which would lead to higher-performance flexible dielectric materials.

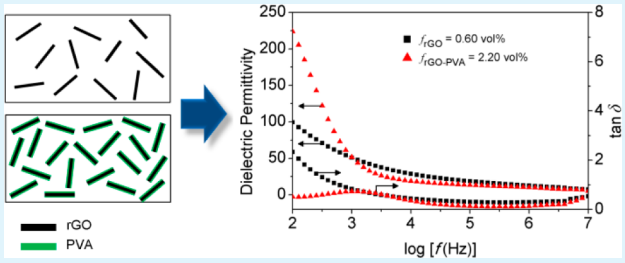

KEYWORDS: *nanocomposite, graphene, poly(vinylidene fluoride), poly(vinyl alcohol), interface, dielectric permittivity*

1. INTRODUCTION

Polymer composites with high dielectric constants (high-ε_r) are highly attractive for their broad range of applications as artificial muscles, charge-storage devices, etc.[1−3] High-ε_r composites are conventionally prepared by blending polymer materials with ferroelectric metal oxides such as $BaTiO_3$ and $Pb(Zr,Ti)O_3$. The dielectric properties of as-prepared composites are a good compromise of the ceramic fillers and the polymer host. However, a relatively high ceramic loading (>50 vol %) is often needed to achieve high-ε_r because of the giant difference between the dielectric constants of inorganic and polymeric materials, which would result in many shortcomings such as poor processability, mechanical brittleness, and high defect density.[4] To overcome these problems, conductive fillers, including metal nanoparticles, carbon nanotubes, and carbon fibers have recently employed to prepare high-ε_r composite materials based on the percolation phenomenon.[4,5] The dielectric properties of composites experience a sharp change when the content of conductive fillers reaches a certain threshold which is usually much lower than 50 vol %.

Poly(vinylidene fluoride) (PVDF) is a semicrystalline thermoplastic polymer with remarkable high piezo- and pyroelectric coefficient, excellent thermal stability and chemical resistance. Recently, many efforts have been devoted to the development of high-ε_r composites based on PVDF and its derivative copolymers. Nan et al. have first reported on the preparation of high-ε_r PVDF-based composites filled with conductive nickel powders.[6] The percolation volume fraction was evaluated to be 17 vol % and the effective ε_r of the composites near the threshold increased to 400 at low frequency. The percolation threshold is strongly dependent on the filler morphology. Theoretically, spherical particles are relatively difficult to reach percolation as compared to those with larger aspect ratio.[5] Indeed, high-ε_r PVDF composites with lower threshold can be obtained by using carbon nanotube as the conductive filler. Our group reported a kind of carbon

Received: September 3, 2012
Accepted: October 31, 2012
Published: October 31, 2012

nanotube/PVDF composite with dielectric constant of 600 at 10^3 Hz when the content of filler is near the critical concentration of 8.0 vol %.[7] Recently, two-dimensional graphene nanosheets have emerged as an even better conductive filler than carbon nanotubes, owing to their ultrahigh aspect ratio, excellent electrical conductivity, and relatively low production cost.[8,9] There are several reports of PVDF-based composites blending with graphene. For instance, Giannelis et al. have first reported the PVDF nanocomposites filled with thermally reduced graphene oxide (TRG).[10] A low percolation threshold of 2 wt % was obtained and the storage modulus and electric conductivity of the composites increased with the TRG concentration. Fan et al. have also reported the TRG/PVDF nanocomposite films prepared by a solution-cast and hot-press method.[11] In this composite material, TRG nanoplates with thickness of 20−60 nm were homogenously dispersed in PVDF matrix with an extremely low percolation threshold of 1.01 vol %. Near the percolation threshold, high-ε_r of 200 and 2700 at 10^3 and 10^2 Hz respectively could be achieved. It should be mentioned that the TRG, which is produced by rapid heating of graphite oxide under inert gas and high temperature, just the same as chemically reduced graphene (CRG), is not real "graphene" but chemically modified graphene (CMG) with structural defects on its basal plane.[9,12] Nanocomposites with isolated monolayer reduced graphene oxide (rGO) sheets dispersed in PVDF matrix have been fabricated by Sodano et al. through a facile and highly efficiently in situ thermal reduction method.[13] The ε_r of the rGO/PVDF reached ca. 100 at the percolation threshold of 1.6 vol %. Very recently, Zhong et al. have also reported rGO/PVDF nanocomposites fabricated through a solution casting approach, which shows a percolation threshold as low as 0.18 vol % and a high-ε_r of 340 at 10^2 Hz near the percolation threshold.[14]

Despite the success of several studies in development of high-ε_r graphene/PVDF nanocomposites, there are still some challenges. First, it is rather difficult to tailor the dielectric properties of the composites by adjusting the volume fraction of graphene, inasmuch as a tiny change in the concentration of conductive filler would cause a dramatic variation of percolation network near the percolation threshold. Second, the dielectric loss (tan δ) in the conductive filler/polymer composites always appears to be very large due to the leakage current among the conductive fillers. Third, poor compatibility between the nonpolar graphene and polar PVDF impedes the formation of a homogeneous composite which leads to the adverse excessive agglomeration of graphene and vacancies at interface. All these negative factors would more or less limit the practical application of graphene/PVDF nanocomposites as high-ε_r materials. To solve these problems, it is obvious that the controllable dispersibility of graphene in the PVDF matrix should be primarily realized. The surface functionalization of graphene nanosheets plays an key role to control their dispersibility throughout a polymer matrix.[8,9,15,16] Recently several reports[17,18] have shown that graphene oxide (GO) or rGO platelets can be well-dispersed into PVDF host by modification of graphene surfaces with poly(methyl methacrylate) (PMMA) chains through surface-initiated atom transfer radical polymerization (SI-ATRP) technique.[19] PVDF and PMMA are completely miscible in melt state[20,21] and thus PMMA chains covalently anchored on graphene surfaces could afford strong interaction between the graphene and PVDF, leading to a steady and homogeneous distribution of graphene throughout the composite.

Along this line, here we report the preparation and dielectric properties of PVDF-based nanocomposites filled with poly(vinyl alcohol)-grafted graphene (rGO-PVA). PVA, though immiscible with PVDF, can form stable intermolecular hydrogen bonds between the hydroxy groups on PVA chains and the fluoride atoms of PVDF chains.[22,23] The hydrogen bond interaction between rGO-PVA and PVDF can stabilize the dispersion of nanofillers in polymer host. The PVA insulating layers on graphene surfaces can also prevent the direct contact of conductive graphene nanosheets, partially reduce the leakage current and thus the dielectric loss. Furthermore, the PVA functionalized graphene can be conveniently prepared through esterification between the hydroxyls of PVA and carboxyl acid groups of GO via a "graft-to" approach,[24−26] avoiding the complicated syntheses process. The chemical structure and morphology of the obtained rGO-PVA were carefully characterized. The microstructure and dielectric properties of PVDF-based nanocomposites filled with modified rGO (rGO-PVA) and original rGO, respectively, are discussed in detail.

2. EXPERIMENTAL SECTION

2.1. Materials and Characterization. PVDF powder (FR903) was purchased from Shanghai 3F New Material Co. Ltd. with the melt flow rate of 2 g/10 min. PVA (PVA 1797) was obtained from Aladdin Chemistry Co. Ltd. with the polymerization degree of 1700 and the alcoholysis degree of 97 mol %. Graphite powder (GP, Sinopharm Chemical Reagent Co. Ltd.) with the size of 300−400 mesh was sieved out prior to use. All other chemicals were obtained as analytical grade products and used without further purification.

Fourier transform infrared (FT-IR) spectra were measured using a Nicolet 5700 spectrometer by incorporating the sample in a KBr disk. Raman spectra were recorded on a Renishaw RM 1000 confocal system spectrometer equipped with an integral microscope and He−Ne laser (633 nm) as the excitation source. Thermal gravimetric analysis (TGA) of the samples was carried out by using TA Instruments TGA 2050 with a heating rate of 10 °C/min under nitrogen atmosphere. AFM images were obtained by using Nanoscople-IIIa scanning probe microscope in the tapping mode. The scanning electron microscope (SEM) observation was performed on a Hitachi S-4700 microscope with an accelerating voltage of 20 kV. The samples were frozen in liquid nitrogen and the resulting freshly fractured surfaces were examined. X-ray diffraction (XRD) analysis was carried out with a Rigaka D/max 2500 diffractometer using a Cu K_α radiation source. Dielectric properties of the nanocomposites were measured using an Agilent 4294A impedance analyzer system. Thin film samples, approximately 1 cm^2 in area with a thickness of ca. 50 μm, onto which silver electrodes had been painted, were tested.

2.2. Preparation of GO-PVA. Graphite oxide was first prepared using a modified Hummers method[27,28] from natural graphite powders and purified by dialysis. The detailed preparation procedures can be found in the Supporting Information. The functionalized GO with PVA covalently bonded on surface, which was designated as GO-PVA, was prepared from the graphite oxide by esterification following the literature method.[24] In a typical process, graphite oxide (0.04 g) and PVA (0.4 g) were dispersed in dimethyl sulfoxide (DMSO, 20 mL) in a round-bottom flask with stirring and sonication. Then, a solution of N,N-dicyclohexylcarbodiimide (DCC, 1.85 g, 9 mmol) and 4-dimethylaminopyridine (DMAP, 0.135 g, 1.1 mmol) in DMSO (20 mL) was added into the flask. The mixture was vigorously stirred at room temperature for 48 h and precipitated into 200 mL of ethanol. The crude product was filtrated and further purified by dissolving in hot water and then precipitating in ethanol for several times. The gray solid obtained was dried under vacuum at 60 °C for 24 h to give the

final product. The weight fraction of PVA in GO-PVA (φ_{PVA}) was estimated as 25% according to TGA results.

2.3. Preparation of of rGO-PVA/PVDF and rGO/PVDF Films. For the preparation of PVDF-based composites filled with PVA-functionalized graphene platelets (rGO-PVA), a desired amount of GO-PVA and 2.0 g of PVDF were first dispersed in 20 mL of N,N-dimethylformamide (DMF) to form homogeneous dispersions by sonication and heating. Reduction of GO-PVA was then carried out by using hydrazine (0.2 mL) at 90 °C for 4 h. After being cooled to room temperature, the mixture was casted onto clean glass slides and dried under vacuum at 80 °C for 24 h to form thin films with thicknesses of ca. 50 μm. The volume fraction of rGO-PVA (f_{vol}) in the composite can be determined by the following equation

$$f_{vol} = \frac{\varphi_{wt}[y(1-\varphi_{PVA})/\rho_G + \varphi_{PVA}/\rho_{PVA}]}{\varphi_{wt}[y(1-\varphi_{PVA})/\rho_G + \varphi_{PVA}/\rho_{PVA}] + (1-\varphi_{wt})/\rho_{PVDF}} \times 100\% \quad (1)$$

where φ_{wt} represents the weight fraction of GO-PVA in GO-PVA/PVDF mixture; φ_{PVA} (= 25%) means the weight fraction of PVA in GO-PVA hybrid material; y is the reduction yield of graphene reduced from graphite oxide, which was estimated to be 0.46 according to TGA results; ρ_G, ρ_{PVA}, and ρ_{PVDF} are the density of graphite (2.28 g/cm^3), PVA (1.27 g/cm^3) and PVDF (1.78 g/cm^3), respectively.

The preparation procedure of rGO/PVDF films was similar to that of rGO-PVA/PVDF films, using graphite oxide to displace GO-PVA. The volume content of rGO in rGO/PVDF composite can also be calculated through eq 1 by setting φ_{PVA} = 0.

3. RESULTS AND DISCUSSION

GO platelets functionalized with PVA (GO-PVA) were first prepared as a precursor for the further generation of conductive fillers. It is well-known that the chemically derived GO contains large amounts of epoxy groups and hydroxyls on its basal plane and carboxyls on the edge.[12,29,30] Here the GO-PVA was obtained through esterification between the carboxyls of GO and the hydroxyls on PVA chains.[24,26] The chemical structure of as-obtained GO-PVA was carefully characterized by FT-IR and Raman spectroscopy (see Figure S1 in the Supporting Information). Figure 1 shows the FT-IR spectra of GO and

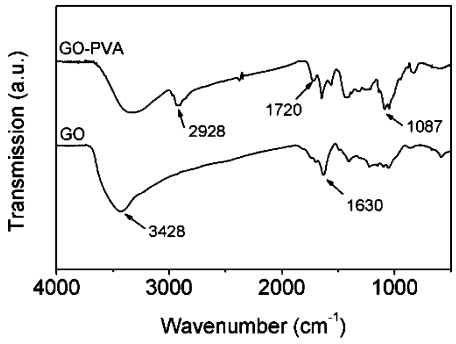

Figure 1. FT-IR spectra of GO and GO-PVA.

GO-PVA. In the spectrum of GO, the peaks at 3428 and 1630 cm^{-1} are related to the −OH and C═C bonds, respectively. After the PVA functionalization, these bonds were intact, and thus the corresponding peaks did not change significantly. The peak at 1720 cm^{-1}, which can be attributed to C═O stretching of ester groups, increased remarkably after functionalization, indicating the formation of ester bonds. In addition, large intensity peaks at 2928 and 1087 cm^{-1} can be observed after functionalization. These peaks can be attributed to the stretching of C−H and C−O bonds of PVA. The appearance of these peaks suggests that PVA chains have been covalently grafted onto GO platelets successfully.

The morphology of GO and GO-PVA spin-coated on silicon substrates was characterized by AFM, and typical images are shown in Figure 2. It can be seen that an individual sheet of GO

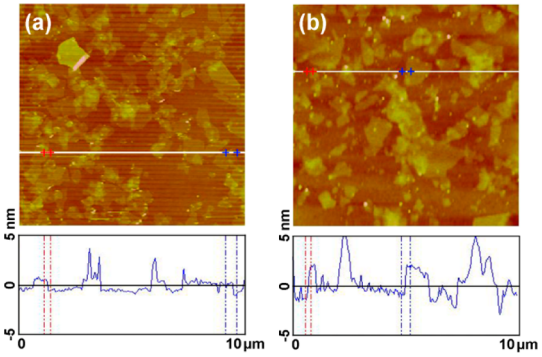

Figure 2. Typical AFM images of (a) GO and (b) GO-PVA deposited on silicon wafer.

has a thickness of ca. 1 nm, which is significantly larger than that of ideal graphene owing to the presence of oxygen-containing functional groups and absorbed water above and below the carbon basal plane.[12] In contrast to the starting GO, the average thickness of single-layered GO-PVA increases to ca. 3.1 nm with a flat surface profile, which indicates that the GO nanosheets are uniformly wrapped by PVA chains. On the other hand, the lateral dimensions of GO and GO-PVA vary from a few nanometers to several micrometers.

The presence of PVA on the graphene nanosheets was further analyzed using TGA by heating under a nitrogen atmosphere to 800 °C at a rate of 10 °C/min. As shown in Figure 3, the thermal gravimetric curve of GO exhibits two

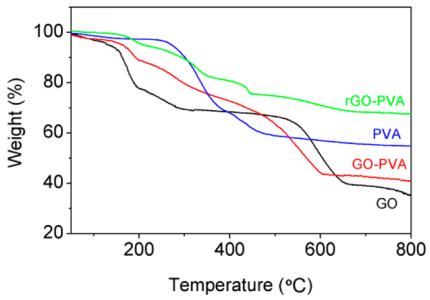

Figure 3. TGA curves of GO, PVA, GO-PVA, and rGO-PVA with a heating rate of 10 °C/min in nitrogen.

rapid weight loss process in the range of 100−300 °C and 500−650 °C, which can be attributed to the decomposition of labile oxygen-containing groups and carbon backbone, respectively.[31] PVA, however, shows only one rapid weight loss process in the temperature range of 250−500 °C. The thermogravimetric curve of GO-PVA can be regarded as the linear addition of GO and PVA. Therefore, the content of PVA in GO-PVA was calculated to be 25 wt % based on the overall weight loss values of GO (65%), PVA (45%), and GO-PVA (60%). This weight fraction value is consistent with that of PVA-grafted GO reported in a recent literature.[26] Furthermore, the thermal stability of GO-PVA is significantly improved after hydrazine reduction for 4 h at 90 °C. The weight loss of resulting rGO-PVA decreases to be 33%. Assuming that the thermal

dx.doi.org/10.1021/am3018652 | ACS Appl. Mater. Interfaces 2012, 4, 6273−6279

degradation residues of GO-PVA and rGO-PVA after TGA experiments are the same, one can calculate the reduction yield from GO to rGO to be 46% under such condition.

According to the percolation theory,[5] the dielectric and conductive properties of composites change sharply near the percolation threshold. To reach the percolation threshold, PVDF films containing different volume contents of rGO-PVA or rGO were fabricated. The composite films were prepared by using solution cast technique. Desired amount of GO-PVA or GO was first mixed with PVDF in DMF solution. After the in situ reduction of GO-PVA or GO by hydrazine, the slurry was casted on precleaned glass substrate to form composite film by evaporating DMF. Though a little more complex than melt blending, the solution blending approach has been proved to achieve a better dispersion of graphene nanosheets in polymer matrix.[9,32,33] Figure 4a and 4b show the SEM images of fracture

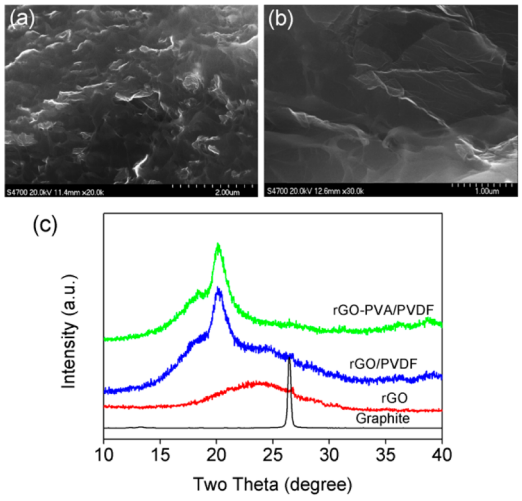

Figure 4. Characteristics of rGO/PVDF and rGO-PVA/PVDF nanocomposites: SEM images of fracture surfaces of (a) rGO-PVA/PVDF (f = 2.20 vol %) and (b) rGO/PVDF (f = 0.60 vol %). (c) XRD patterns of graphite, rGO, rGO/PVDF (f = 0.60 vol %), and rGO-PVA/PVDF (f = 2.20 vol %).

surfaces of rGO-PVA/PVDF and rGO/PVDF nanocomposites. Figure 4a shows that individual rGO-PVA nanosheets are well-dispersed throughout the PVDF matrix. Polymer adhesion to the pulled out rGO-PVA sheets can also be observed due to the strong interfacial interaction between the filler and the PVDF matrix. In contrast, as shown in Figure 4b, the rGO/PVDF composite shows large rGO agglomerations indicating a poor dispersion of rGO in PVDF. The dispersion state of rGO-PVA and rGO in the PVDF matrix was also examined by XRD. The emergence of a shoulder peak at 24° in the XRD pattern of rGO/PVDF nanocomposite (as shown in Figure 4c) clearly demonstrates that some rGO nanosheets restacked together forming a graphite-like structure. The shoulder peak cannot be detected in the XRD pattern of rGO-PVA/PVDF, suggesting that rGO-PVA nanosheets can uniformly disperse in PVDF without discernible aggregation.

It has long been known that the nanofiller dispersion in the polymer matrix is crucial to the electrical, mechanical, thermal, and other properties of nanocomposites. Favorable nanofiller–polymer interactions promote better dispersion of the nanofiller in the polymers, and this is empirically associated with higher effective dielectric constants of the nanocomposites. To further prove the strong interfacial interaction existing between the rGO-PVA nanosheets and the PVDF matrix, FT-IR and Raman experiments were performed. FT-IR spectra of PVA, PVDF, and PVDF nanocomposites filled with rGO-PVA or rGO are shown in Figure 5a. In the spectrum of PVA, the peak at 3425

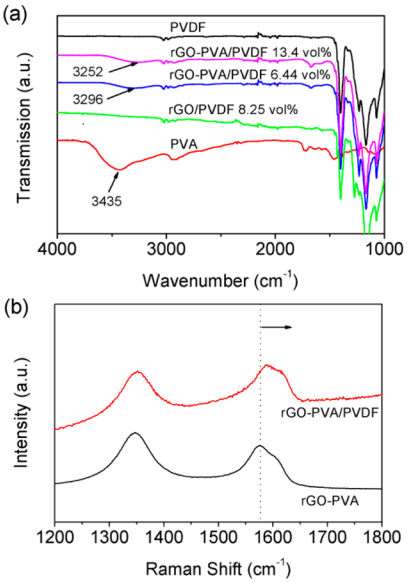

Figure 5. (a) FT-IR spectra of different polymer and nanocomposite samples; (b) Raman spectra of rGO-PVA and PVDF nanocomposite with 2.20 vol % of rGO-PVA.

cm^{-1} is ascribed to the O–H stretching vibration. In the case of rGO-PVA/PVDF nanocomposites, this O–H stretch appears at lower energy position. For the nanocomposite filled with 6.44 vol % of rGO-PVA, the O–H vibration peak occurred at 3296 cm^{-1}. This peak further moved to 3252 cm^{-1} when the nanofiller content increased to 13.4 vol %. The reduction of O–H vibration energy suggests the formation of more stable hydrogen bonds. Meanwhile, no O–H stretch peak can be detected in pure PVDF and rGO/PVDF nanocomposites, indicating that the strong hydrogen bonds are mainly formed between –OH groups of PVA on rGO-PVA nanosheet surface and fluoride atoms of PVDF. Figure 5b gives the Raman spectra of rGO-PVA and rGO-PVA/PVDF with filler content of 2.20 vol %. For the spectrum of rGO-PVA, the prominent peaks at 1350 and 1574 cm^{-1} correspond to the well-documented D and G bands of graphene.[34] After dispersed in PVDF matrix, the G band shifted to higher frequency side while the D band position did not change. The blue shift of the G band is mainly caused by charge doping with electron-withdrawing components of PVDF.[35] The IR and Raman results clearly evidence the strong interaction between rGO-PVA nanosheets and PVDF. Both the hydrogen bonding and the charge transfer effect are benefit to stabilize the dispersion of rGO-PVA in PVDF matrix.

Panels a and b in Figure 6 show the variations of dielectric permittivity of rGO-PVA/PVDF and rGO/PVDF nanocomposite films with the alternating electric field frequency at room temperature, respectively. A common feature that can be seen in both figures is that the addition of rGO-PVA or rGO increases the dielectric permittivity of PVDF host, which is consistent with other percolative nanocomposites filled by carbon nanotubes or graphene nanosheets.[4,7,11,13,14] The promotion in dielectric permittivity can be mainly attributed to a gradual formation of microcapacitor networks in the PVDF matrix as the volume fraction of conductive nanofiller

dx.doi.org/10.1021/am3018652 | ACS Appl. Mater. Interfaces 2012, 4, 6273–6279

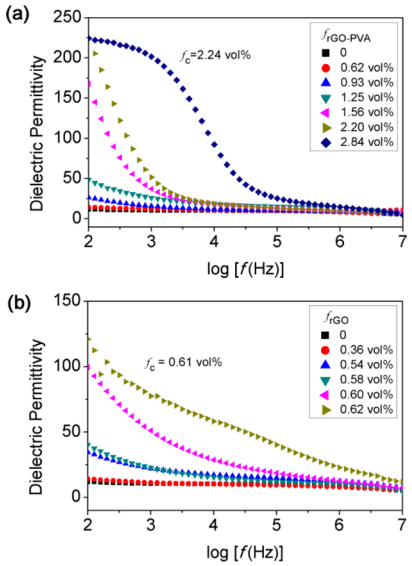

Figure 6. Dependence of dielectric permittivity of (a) rGO-PVA/PVDF films and (b) rGO/PVDF films with different filler contents on the alternating electric field frequency at room temperature.

increases.[7,11] The microcapacitors consist of rGO-PVA or rGO nanoplatelets separated by a thin insulating PVDF layer. For the composites filled with conductive fillers, the percolation theory depicts that the variations of dielectric constant with frequency follows a power law as the filler content approaches percolation threshold. In our composite system, the power law can be expressed by the following equation[5]

$$\varepsilon_{\text{eff}} \propto \varepsilon_{\text{PVDF}}(f_c - f)^{-s} \text{ for } f < f_c \quad (2)$$

where ε_{eff} represents the dielectric constant of composites, $\varepsilon_{\text{PVDF}}$ is the dielectric constant of PVDF, f is the volume fraction of filler, f_c is the percolation threshold and s is the critical exponent. The numerical fitting of the experimental data according to the eq 2 gives f_c(rGO-PVA) = 2.24 vol % and f_c(rGO) = 0.61 vol %. Generally, a low percolation threshold is expected to maintain the mechanical flexibility of polymer matrix. The percolation threshold of rGO/PVDF nanocomposites, 0.61 vol %, is much lower than that of PVDF nanocomposites filled with carbon nanotubes (~8 vol %).[7] This value is also lower than that of graphene/PVDF nanocomposites (~ 1 vol %), in which the graphene was prepared through a thermal reduction approach,[11] but higher than that of recently reported rGO/PVDF nanocomposites (~ 0.18 vol %) in which the rGO was obtained by phenylhydrazine reduction from GO.[14] The percolation threshold is strongly dependent on the distribution of fillers in a matrix, which can be influenced by the particles shape, size, orientation, etc.[5] Apparently, lower threshold values can be readily achieved by using chemically reduced GO as the filler. The ultralow thresholds are mainly attributed to the two-dimensional planar structure and extremely high aspect ratio of chemically reduced GO. In contrast, the percolation threshold of rGO-PVA/PVDF nanocomposites goes up to 2.24 vol %, indicating that the surface modification makes the percolative network of rGO harder to achieve. It is reasonable because the PVA chains covalently anchored on rGO can slightly decrease the conductivity and prevent the direct contact of the conductive nanosheets.

To further understand the effect of the PVA shell on the dielectric properties, we compared nanocomposites filled with 0.60 vol % of rGO and 2.20 vol % of rGO-PVA. Both of the filler contents in the samples are slightly less than the percolation threshold. As shown in Figure 7, the dielectric

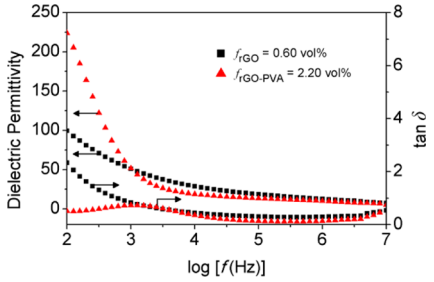

Figure 7. Frequency dependence of dielectric permittivity and loss factor of rGO/PVDF and rGO-PVA/PVDF nanocomposites with the filler volume fraction near the percolation threshold.

permittivity of the samples decreases exponentially with an increase in frequency at low-frequency region (1×10^2 to 1×10^5 Hz). When the frequency is greater than 1×10^5 Hz, the dielectric permittivity attains a relatively stable value. The frequency dependence behavior of the dielectric constants in the low-frequency range should be mainly ascribed to the Maxwell–Wagner–Sillars (MWS) polarization.[7,11] MWS polarization, also known as interfacial polarization, occurs whenever there is an accumulation of charge carriers at an interface between two materials. Near the percolation threshold, conductive rGO or rGO-PVA nanosheets are almost touching each other but still remaining insulative due to the existence of a PVDF space layer. Therefore, the free charges in graphene pile up at the interface and give rise to the strong MWS polarization, and thus lead to the increase in the dielectric constant. It is noted that the rGO-PVA/PVDF nanocomposite exhibits higher dielectric constants and smaller loss factor than that of rGO/PVDF at lower frequency region (<1×10^3 Hz). At 1×10^2 Hz, the dielectric constants of rGO-PVA/PVDF and rGO/PVDF are about 230 and 100, respectively. However, the dielectric constants of both composites get very close to each other when the frequency increases to 1×10^3 Hz. Apparently, the dielectric permittivity of rGO-PVA/PVDF composite shows an even more serious frequency dependence behavior, suggesting that there should be a stronger MWS polarization. A recent report concerning the dielectric properties of graphene/PVA nanocomposites has demonstrated that a strong MWS polarization exists between graphene nanosheets and PVA matrix.[36] In current work, the introduction of PVA covalently bonded on rGO makes the interface between rGO and PVDF more sophisticated. But anyhow, the percolation threshold was improved for rGO-PVA/PVDF composites. Thus near the percolation threshold more nanofillers were blended into PVDF, which led to more interface area and enhanced the MWS polarization. Furthermore, the insulating PVA chains grafted on graphene surface can prevent the direct contact of the conductive rGO-PVA. That is conducive to minimizing the leakage current in composite and reduce the dielectric loss. Dielectric properties of PVDF-based nanocomposites incorporated with various graphene nanosheets in literature are also summarized in Table S2 (see the Supporting Information). Compared with other nanocomposite systems, a relatively high dielectric constant (230) together with a satisfied loss factor (0.5) are simultaneously achieved in current rGO-PVA/PVDF nanocomposites.

dx.doi.org/10.1021/am3018652 | ACS Appl. Mater. Interfaces 2012, 4, 6273–6279

It should be also mentioned that a broad peak centered at about 1×10^3 Hz is visible on dielectric loss curve of rGO-PVA/PVDF nancomposites near the percolation threshold. This relaxation peak should be ascribed to the MWS polarization mechanism. However, in rGO/PVDF nanocomposite, the relaxation peak corresponds to MWS polarization resides in a lower frequency region, which exceeds the measurement limit and cannot be seen in the figure. This result reveals that the accumulated charges at the rGO-PVA/PVDF interfaces exhibit a shorter relaxation time than in rGO/PVDF system. It is believed that a better adhesion of graphene onto electrodes can significantly reduce contact resistance and improve carrier mobilities.[37] Therefore we speculate that the hydrogen bond and other interactions between rGO-PVA and PVDF matrix enhance the adhesion and result in a faster mobility of interface charges, i.e. a shorter relaxation time.

An excellent property of a dielectric material is not only its ability to increase capacitance, but also, and equally important, its insulating behavior. The low conductivity is often needed to prevent the charge conduction from one electrode plate to another. Figure 8 displays the frequency dependence of

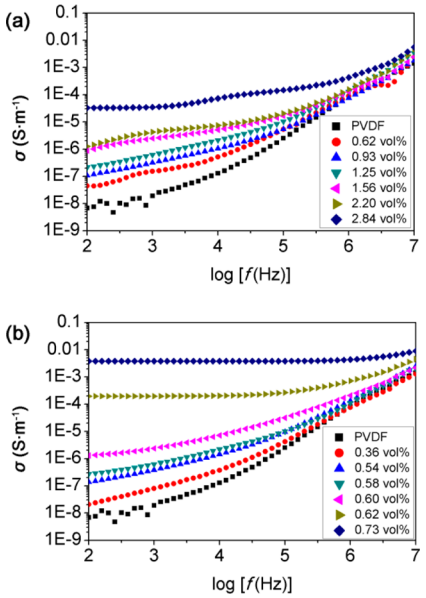

Figure 8. Dependence of electrical conductivity of (a) rGO-PVA/PVDF films and (b) rGO/PVDF films with different filler contents on the alternating electric field frequency at room temperature.

alternating current (AC) conductivity of rGO-PVA/PVDF and rGO/PVDF nanocomposites with different filler contents in the 1×10^2 to 1×10^7 Hz range. It can be clearly seen that both composite systems show typical percolation transition as the filler content increases. For rGO/PVDF nanocomposites, the conductivity shows strong dependence on frequency at low rGO contents owing to the insulating nature. Although the conductivity displays a conducting characteristic which remains nearly frequency-independent when the rGO loading exceeds the percolation threshold (0.61 vol %). The frequency-independent conductivity is commonly regarded as direct current (DC) conductivity. With 0.73 vol % loading of rGO, the DC conductivity of rGO/PVDF composite reaches to ca. 3.8×10^{-3} S/m. Similar to rGO/PVDF system, composites filled with rGO-PVA also show an obvious insulator-to-conductor transition. However, the AC conductivity still presents frequency dependent behavior even if the rGO-PVA contents exceed the percolation threshold. For instance, the conductivity of composite containing 2.84 vol % of rGO-PVA remains stable (ca. 4.0×10^{-5} S/m) in the lower-frequency region and becomes frequency-dependent approaching 1×10^4 Hz.

4. CONCLUSIONS

In this study, PVDF-based nanocomposites filled with conductive rGO-PVA and rGO were prepared and characterized. FT-IR and AFM results demonstrated that PVA chains have been successfully grafted onto graphene nanosheets. The additional PVA plays an important role in the enhancement of composite properties. Hydrogen bonds between PVA and PVDF lead to a better dispersion of rGO-PVA in matrix. The values of percolation threshold for rGO/PVDF and rGO-PVA/PVDF were determined to be 0.61 vol % and 2.24 vol %, respectively. Compared with the rGO/PVDF composites, higher dielectric permittivity together with lower loss factor are achieved in rGO-PVA/PVDF nanocomposites in frequency range of 1×10^2 to 1×10^3 Hz. At 1×10^2 Hz, the rGO-PVA/PVDF nanocomposite (f(rGO-PVA) = 2.20 vol %) shows a high dielectric constant of 230, which is 2.3 times higher than that of rGO/PVDF nanocomposite (f(rGO) = 0.60 vol %). The modification of graphene/polymer interface makes the flexible rGO-PVA/PVDF nanocomposites more attractive for practical applications in energy storage devices.

■ ASSOCIATED CONTENT

Ⓢ Supporting Information

Detailed synthesis procedures of graphite oxide, Raman spectra, summary of dielectric properties of various PVDF-based nanocomposites. This material is available free of charge via the Internet at http://pubs.acs.org.

■ AUTHOR INFORMATION

Corresponding Author

*E-mail dangzm@ustb.edu.cn (Z.-M.D.); guo-hua.hu@univ-lorraine.fr (G.-H.H.).

Notes

The authors declare no competing financial interest.

■ ACKNOWLEDGMENTS

The financial support from the NSFC (51103011, 51073015), the Fundamental Research Funds for the Central Universities (FRF-TP-11-003B), and the Ministry of Sciences and Technology of China through China-Europe International Incorporation Project (2010DFA51490) is gratefully acknowledged.

■ REFERENCES

(1) Mirfakhrai, T.; Madden, J. D. W.; Baughman, R. H. *Mater Today* **2007**, *10*, 30−38.
(2) Brochu, P.; Pei, Q. B. *Macromol. Rapid Commun.* **2010**, *31*, 10−36.
(3) Barber, P.; Balasubramanian, S.; Anguchamy, Y.; Gong, S.; Wibowo, A.; Gao, H.; Ploehn, H.; Loye, H. *Materials* **2009**, *2*, 1697−1733.
(4) Dang, Z. M.; Yuan, J. K.; Zha, J. W.; Zhou, T.; Li, S. T.; Hu, G. H. *Prog. Mater. Sci.* **2012**, *57*, 660−723.
(5) Nan, C. W. *Prog. Mater. Sci.* **1993**, *37*, 1−116.
(6) Dang, Z. M.; Lin, Y. H.; Nan, C. W. *Adv. Mater.* **2003**, *15*, 1625−1629.

(7) Dang, Z. M.; Wang, L.; Yin, Y.; Zhang, Q.; Lei, Q. Q. *Adv. Mater.* **2007**, *19*, 852−857.
(8) Kuilla, T.; Bhadra, S.; Yao, D.; Kim, N. H.; Bose, S.; Lee, J. H. *Prog. Polym. Sci.* **2010**, *35*, 1350−1375.
(9) Kim, H.; Abdala, A. A.; Macosko, C. W. *Macromolecules* **2010**, *43*, 6515−6530.
(10) Ansari, S.; Giannelis, E. P. *J. Polym. Sci. B Polym. Phys.* **2009**, *47*, 888−897.
(11) He, F.; Lau, S.; Chan, H. L.; Fan, J. T. *Adv. Mater.* **2009**, *21*, 710−715.
(12) Dreyer, D. R.; Park, S.; Bielawski, C. W.; Ruoff, R. S. *Chem. Soc. Rev.* **2010**, *39*, 228−240.
(13) Tang, H. X.; Ehlert, G. J.; Lin, Y. R.; Sodano, H. A. *Nano Lett.* **2012**, *12*, 84−90.
(14) Fan, P.; Wang, L.; Yang, J.; Chen, F.; Zhong, M. *Nanotechnology* **2012**, *23*, 365702.
(15) Xu, Z.; Gao, C. *Macromolecules* **2010**, *43*, 6716−6723.
(16) Kan, L.; Xu, Z.; Gao, C. *Macromolecules* **2011**, *44*, 444−452.
(17) Goncalves, G.; Marques, P. A. A. P.; Barros-Timmons, A.; Bdkin, I.; Singh, M. K.; Emami, N.; Gracio, J. *J. Mater. Chem.* **2010**, *20*, 9927−9934.
(18) Layek, R. K.; Samanta, S.; Chatterjee, D. P.; Nandi, A. K. *Polymer* **2010**, *51*, 5846−5856.
(19) Braunecker, W. A.; Matyjaszewski, K. *Prog. Polym. Sci.* **2007**, *32*, 93−146.
(20) Mijovic, J.; Sy, J. W.; Kwei, T. K. *Macromolecules* **1997**, *30*, 3042−3050.
(21) Sy, J. W.; Mijovic, J. *Macromolecules* **2000**, *33*, 933−946.
(22) Yano, S.; Iwata, K.; Kurita, K. *Mater. Sci. Eng. C* **1998**, *6*, 75−90.
(23) Bhajantri, R. F.; Ravindrachary, V.; Harisha, A.; Crasta, V.; Nayak, S. P.; Poojary, B. *Polymer* **2006**, *47*, 3591−3598.
(24) Salavagione, H. J.; Gomez, M. A.; Martinez, G. *Macromolecules* **2009**, *42*, 6331−6334.
(25) Veca, L. M.; Lu, F. S.; Meziani, M. J.; Cao, L.; Zhang, P. Y.; Qi, G.; Qu, L. W.; Shrestha, M.; Sun, Y. P. *Chem. Commun.* **2009**, 2565−2567.
(26) Cheng, H. K. F.; Sahoo, N. G.; Tan, Y. P.; Pan, Y.; Bao, H.; Li, L.; Chan, S. H.; Zhao, J. *ACS Appl. Mater. Interfaces* **2012**, *4*, 2387−2394.
(27) Hummers, W. S.; Offeman, R. E. *J. Am. Chem. Soc.* **1958**, *80*, 1339−1339.
(28) Bai, H.; Xu, Y. X.; Zhao, L.; Li, C.; Shi, G. Q. *Chem. Commun.* **2009**, 1667−1669.
(29) Park, S.; Ruoff, R. S. *Nat. Nanotechnol.* **2009**, *4*, 217−224.
(30) Loh, K. P.; Bao, Q. L.; Ang, P. K.; Yang, J. X. *J. Mater. Chem.* **2010**, *20*, 2277−2289.
(31) Jeong, H. K.; Lee, Y. P.; Jin, M. H.; Kim, E. S.; Bae, J. J.; Lee, Y. H. *Chem. Phys. Lett.* **2009**, *470*, 255−258.
(32) Stankovich, S.; Dikin, D. A.; Dommett, G. H. B.; Kohlhaas, K. M.; Zimney, E. J.; Stach, E. A.; Piner, R. D.; Nguyen, S. T.; Ruoff, R. S. *Nature* **2006**, *442*, 282−286.
(33) He, F. A.; Fan, J. T.; Lau, S. T. *Polym. Test.* **2008**, *27*, 964−970.
(34) Zhu, Y. W.; Murali, S.; Cai, W. W.; Li, X. S.; Suk, J. W.; Potts, J. R.; Ruoff, R. S. *Adv. Mater.* **2010**, *22*, 3906−3924.
(35) Das, B.; Voggu, R.; Rout, C. S.; Rao, C. N. R. *Chem. Commun.* **2008**, 5155−5157.
(36) Tantis, I.; Psarras, G. C.; Tasis, D. *eXPRESS Polym. Lett.* **2012**, *6*, 283−292.
(37) Wang, S. A.; Ang, P. K.; Wang, Z. Q.; Tang, A. L. L.; Thong, J. T. L.; Loh, K. P. *Nano Lett.* **2010**, *10*, 92−98.